Nigerian Journal of Engineering, Vol. 29, No. 1, April 2022, ISSN (print): 0794 – 4756, ISSN(online):2705-3954.

Nigerian Journal of Engineering,
Faculty of Engineering, Ahmadu Bello University, Zaria, Nigeria
journal homepage: www.njeabu.com.ng

Numerical Simulation of Change in Reservoir Properties Arising from Near Oil Wellbore Damages

T. A. Adeosun[1], M. A. Adabanija[2], F.O. Akinpelu[3]

[1]Department of Mineral and Petroleum Engineering, Yaba College of Technology, Lagos – Nigeria.
[2]Department of Earth Sciences, Ladoke Akintola University of Technology, Ogbomoso – Nigeria.
[3]Department of Pure and Applied Mathematics, Ladoke Akintola University of Technology, Ogbomoso – Nigeria.
[1]adebaba2001@yahoo.com

Research Article

Abstract

Long down-time and colossus economic loss associated with frequent well shut down required for proper well test analysis near oil wellbore damages has necessitated the use of numerical models for simulating change in reservoir properties. In the current study, change in reservoir properties has been simulated by formulating models involving modification of Darcy equation in an attempt to optimize reservoir pressure for improved reservoir properties. The coupled transient linear partial differential equations (CTLPDE) models developed for predicting reservoir properties such as porosity, permeability and water saturation profile were numerically solved using finite difference method implemented in MATLAB and solution validated using field data perturbed with Gaussian noise of ±10%. The results obtained for CTLPDE models indicated initial decrease in both water and oil pressure from 4550 psi and 350 psi to 4525 psi and 320 psi respectively. Both water and oil pressure subsequently increased to 4530 psi and 325 psi and then remained constant. However, while water saturation (S_w) increased throughout the pressure regime; 0.730 through 0.735 to 0.739, oil saturation (S_o) decreased from 0.320 through 0.268 to 0.263. The results of the corresponding auxiliary equation indicated increase in relative permeability of water (K_{rw}) with S_w but decreased with increase in S_o, while relative permeability of oil (K_{ro}) decreased with increase in S_w but increased with S_o. Generally, however, for every value of either S_o or S_w , $k_{rw} \gg k_{ro}$. Numerical simulation proved to be effective in predicting reservoir behavior. The formulated models indicate drop in oil saturation as pressure depleted over time.

Keywords
Formation damage; Gaussian noise; Long down-time, Shut down; Oil pressure; Water saturation

Article History
Received:– December, 2021
Reviewed:– February, 2022
Accepted:– April, 2022
Published:– April, 2022

1. Introduction

Formation damage in oil wells is any process that causes an undesirable reduction of permeability or reduction in the natural inherent productivity of an oil producing formation (Civan, 2007;Civan, 2015). It is a condition most commonly caused by wellbore fluids used during drilling, well completions, work-over operations and subsequent injection of water, steam, and CO_2 flooding (Civan, 2000; Chen *et al*.,2018). Formation damage could also results in blockage of pore spaces, hindrance of flow assurance and high viscosity (Civan, 2002). Loss of drilling mud to the formation does not have immediate serious consequence. However, if the rate of loss increases or completely lost, then there is likelihood of the existence of loss of reservoir properties such as porosity, permeability, and water saturation. Specifically, permeability has been regarded as the most prominent feature of a damaged formation (Civan, 2003; Abreu*et al.* 2007; Wang *et al*., 2018). Major causes of formation damage include bacterial entrainment, emulsion, mud filtrate invasions, clay swelling, organic wax, scale formation, fine particles migration and loss of reservoir properties (Civan, 2001; Civan2003; Amanda *et al*. 2018).

Well stimulation has been recognized as proper antidote for formation damage based on its capability to enhance reservoir properties by improving the flow of reservoir fluids and increase ultimate economic recovery (Marcelo, *et al.* 2013). However, long down-time and its associated enormous economic loss as a result of frequent well shut down required for proper well test analysis has necessitated the need to develop alternative approach. Numerical simulation, process for inferring reservoir behavior from the behavior of a mathematical model, readily offers a preferred alternative. Numerical reservoir simulation is now a useful tool for stimulating formation damage processes (Civan et al., 2004; Civan, 2007; Lopez, 2011; Ayorinde*et al.* 2018) as well as monitoring flow and fluids transport to describe changes in pressure, saturation and reservoir properties for optimized recovery (Xu*et al*. 2018; Cai and Hu, 2019). However, of all the methods, finite difference method has some important advantages of using implicit pressure and implicit saturation schemes when compared with others (Schneider, 2013; Ma *et al.* 2018). It provides approximate solutions in continuous discrete points in the domain and progressive time steps. In the current study, finite difference method has been used for the

estimation of water saturation during pressure and saturation changes in the reservoir flow problem for homogeneous and isotropic porous media within a regular boundary domain. Although, reservoir pressure during lost circulation is governed by partial differential problems on mass transport phenomena focusing on reservoir engineering problem (Ma *et al.* 2019).

2. Problem Formulation

The Darcy's law can be used together with the mass conservation law and equation of state to obtain coupled linear transient partial differential equation for the prediction of reservoir propertiesof the two-phase flow of liquids in porous and permeable media (Marcelo*et al.,* 2013). The mass conservation law for flow in porous medium is given by

$$\frac{\partial(\phi\rho_n)}{\partial t} = -\nabla.(\rho_n\bar{u}) \tag{1}$$

Where ρ_n is the two-phase fluid density for$n(w,o)$, ϕ is the porosity, $\bar{u}$ is the apparent velocity vector. Darcy's law relates velocity and pressure field as follows:

$$\bar{u} = -\frac{k}{\mu_n}\nabla p \tag{2}$$

With $\bar{u} = (u_x, u_y)$ and $k(\bar{r})$ being the permeability tensor, and $\bar{r}(x,y)$, μ_n is the dynamic viscosity of phase $n$and $q(\bar{n}sc,t)$ is the source term's rate per unit volume representing the production injection well at standard condition. By plugging the Darcy's law, the cross-sectional area (A), into (1), coupled linear transient partial differential equations (CLTPDE) describing the flow of a wetting (water) phase and a non-wetting (oil) phase:

$$\nabla.\left[\frac{Ak(x)k_{rw}}{\mu_w}\nabla(p_w(\bar{r},t) - \rho_w gh\right] + \nabla.\left[\frac{Ak(y)k_{rw}}{\mu_w}\nabla(p_w(\bar{r},t) - \rho_w gh\right] + q_{wsc} = v_b\phi(\bar{r})\frac{\partial s_w}{\partial t} \tag{3}$$

$$\nabla.\left[\frac{Ak(x)k_{ro}}{\mu_o}\nabla(p_o(\bar{r},t) - \rho_o gh\right] + \nabla.\left[\frac{Ak(y)k_{ro}}{\mu_w}\nabla(p_o(\bar{r},t) - \rho_o gh\right] + q_{osc} = v_b\phi(\bar{r})\frac{\partial s_o}{\partial t} \tag{4}$$

In (3) and (4), $\bar{r}$ is the position vector according to orthogonal coordinate system,if the saturation of fluid phase becomes less than the critical value, then it will no longer exist as a continuous phase. Such fluid phase has lost the ability to move then (k_{rw}), the relative permeability to water and oil(k_{ro})becomes zero. Suppose there is one flowing phase only. The immobile phases are compressible and will add to the system compressibility. The total isothermal compressibility of liquids (c_t) and the formation compressibility (c_f) will account for the immobile phases $c_i$is given by:

$$c_t = c_0 s_{oi} + c_w s_{wi} + c_f \tag{5}$$

The CLTPDE model equations is consistent with the addition of auxiliary equation (6) and (7) for the four unknown variables p_o , p_w , s_o , s_w

$$p_{cow}(s_w) = p_{nw} - p_w = p_o - p_w \tag{6}$$

$$s_o + s_w = 1 \tag{7}$$

For two-phases (e.g., water and oil) present in the pore spaces of the porous medium neglecting the gas phase. The current study proposes an implicit pressure implicit saturation scheme (IPIS) of finite difference method of solution for homogeneous and isotropic porous media which is more robust when compared with implicit pressure explicit saturation scheme (IMPES).

3. Solution Methodology

The method of solution in the current study discretizes the CLTPDE for two-phase flow through a homogeneous and isotropic porous medium. Approximates solution to the problem was obtained by dividing the domain into uniform grid for approximately different time step. The physical phenomenon described by CLTPDE, combined with a set of boundary and initial conditions is represented by the following Boundary –Value Problem (BVP):

$$A\frac{k(x)k_{rw}}{\mu_w}\frac{\partial^2 p(x,y,t)}{\partial x^2} + A\frac{k(y)k_{rw}}{\mu_w}\frac{\partial^2 p(x,y,t)}{\partial y^2} + q_{wsc} = v_b\phi\frac{\partial s_w}{\partial t}\begin{matrix}0\le x\le 1\\ 0\le y\le 1\end{matrix} \quad t>0 \tag{8}$$

$$A\frac{k(x)k_{ro}}{\mu_o}\frac{\partial^2 p(x,y,t)}{\partial x^2} + A\frac{k(y)k_{ro}}{\mu_o}\frac{\partial^2 p(x,y,t)}{\partial y^2} + q_{osc} = v_b\phi\frac{\partial s_o}{\partial t}\begin{matrix}0\le x\le 1\\ 0\le y\le 1\end{matrix} \quad t>0 \tag{9}$$

$$\frac{\partial p(x,y,t)}{\partial x} = 0 \qquad \begin{matrix}y=0\\ y=1\end{matrix} \quad t>0 \tag{10}$$

$$\frac{\partial p(x,y,t)}{\partial y} = 0 \qquad \begin{matrix}x=0\\ x=1\end{matrix} \quad t>0 \tag{11}$$

$$p(x,y,0) = p_o = 400 \qquad \begin{matrix}0\le x\le 1\\ 0\le y\le 1\end{matrix} \quad t>0 \tag{12}$$

Solving the coupled equations using implicit pressure–implicit saturation method requires change in saturation and pressure. Discretization was therefore required due its efficient use of algorithm that approximates the solution to a problem. Thus, discretization of the left-hand side of equation (8) and (9) yielded:

$$A_x\frac{\partial}{\partial x}\left[\frac{kK_{rw}}{\mu_w B_w}\frac{\partial}{\partial x}[P_w(x,y,t)]\right] + A_y\frac{\partial}{\partial y}\left[\frac{kK_{rw}}{\mu_w B_w}\frac{\partial}{\partial y}[P_w(x,y,t)]\right] + q_{wsc} = \frac{V_b}{\alpha}\phi\frac{\partial}{\partial t}\left(\frac{S_w}{B_w}\right) \tag{13}$$

and

$$A_x \frac{\partial}{\partial x}\left[\frac{kK_{ro}}{\mu_o B_o}\frac{\partial}{\partial x}[P_o(x,y,t)]\right] + A_y \frac{\partial}{\partial y}\left[\frac{kK_{ro}}{\mu_o B_o}\frac{\partial}{\partial y}[P_o(x,y,t)]\right] + q_{osc} = \frac{V_b}{\alpha}\phi\frac{\partial}{\partial t}\left(\frac{S_o}{B_o}\right) \quad (14)$$

respectively. Using the transmissibility relationship$T_{i,j}$ on the discretization of the left-hand side (LHS) of equation (13) and (14) (Schneider, 2013)

$$\frac{\partial}{\partial x}\left(k\lambda_o\frac{\partial P_o}{\partial x}\right) \approx T_{xoi+\frac{1}{2},j}\left(P_{oi+1,j}-P_{oi,j}\right) + T_{xoi-j}\left(P_{oi-1,j}-P_{oi,j}\right) \quad (15a)$$

$$\frac{\partial}{\partial y}\left(k\lambda_o\frac{\partial P_o}{\partial y}\right) \approx T_{yoi,j+\frac{1}{2}}\left(P_{oi,j+1}-P_{oi,j}\right) + T_{xoi,j-\frac{1}{2}}\left(P_{oi,j-1}-P_{oi,j}\right) \quad (15b)$$

$$\frac{\partial}{\partial x}\left(k\lambda_w\frac{\partial P_w}{\partial x}\right) \approx T_{xwi+\frac{1}{2},j}\left(P_{wi+1,j}-P_{wi,j}\right) + T_{xwi-\frac{1}{2},j}\left(P_{wi-1,j}-P_{wi,j}\right) \quad (15c)$$

$$\frac{\partial}{\partial y}\left(k\lambda_w\frac{\partial P_w}{\partial y}\right) \approx T_{ywi,j+\frac{1}{2}}\left(P_{wi,j+1}-P_{wi,j}\right) + T_{ywi,j-\frac{1}{2}}\left(P_{wi,j-1}-P_{wi,j}\right) \quad (15d)$$

where

$$T_{xoi+\frac{1}{2},j} = \frac{2\lambda_{oj+\frac{1}{2},j}}{\Delta x_{i,j}\left(\frac{\Delta x_{i+1,j}}{K_{i+1,j}}+\frac{\Delta x_{i,j}}{K_{i,j}}\right)},$$

$$T_{yoi+\frac{1}{2}} = \frac{2\lambda_{oi,j+\frac{1}{2}}}{\Delta y_{i,j}\left(\frac{\Delta y_{i,j+1}}{K_{i,j+1}}+\frac{\Delta y_{i,j}}{k_{i,j}}\right)} \quad (16)$$

The discretization of the right-hand side (RHS) of equation (14) for oil is given by

$$\frac{\partial}{\partial t}\left(\frac{\phi S_o}{B_o}\right) = \frac{\phi}{B_o}\frac{\partial S_o}{\partial t} + S_o\frac{\partial}{\partial t}\left(\frac{\phi}{B_o}\right)$$

$$\frac{\partial}{\partial t}\left(\frac{\phi S_o}{B_o}\right) = -\frac{\phi}{B_o}\frac{\partial S_w}{\partial t} + (1-S_w)\left[\phi\frac{\partial}{\partial t}\left(\frac{1}{B_o}\right)+\frac{1}{B_o}\frac{\partial\phi}{\partial t}\right]$$

$$\frac{\partial}{\partial t}\left(\frac{\phi S_o}{B_0}\right) = -\frac{\phi}{B_o}\frac{\partial S_w}{\partial t} + (1-S_w)\left[\phi\frac{\partial\left(\frac{1}{B_o}\right)}{\partial P_o}.\frac{\partial P_o}{\partial t}+\frac{1}{B_o}\frac{\partial\phi}{\partial P_o}.\frac{\partial P_o}{\partial t}\right]$$

$$\frac{\partial}{\partial t}\left(\frac{\phi S_o}{B_o}\right) = -\frac{\phi}{B_o}\frac{\partial S_w}{\partial t} + \phi(1-S_w)\left[\frac{\partial\left(\frac{1}{B_o}\right)}{\partial P_o}+\frac{1}{B_o}\frac{\partial\phi}{\phi\partial P_o}\right]\frac{\partial P_o}{\partial t} \quad (17)$$

Substitute for $C_r = \frac{\partial\phi}{\phi\partial P_o}$ in (17), yielded

$$\frac{\partial}{\partial t}\left(\frac{\phi S_o}{B_o}\right) = -\frac{\phi}{B_o}\frac{\partial S_w}{\partial t} + \phi(1-S_w)\left[\frac{\partial\left(\frac{1}{B_o}\right)}{\partial P_o}+\frac{C_r}{B_o}\right]\frac{\partial P_o}{\partial t} \quad (18)$$

Using backward difference

$$\frac{\partial}{\partial t}\left(\frac{\phi S_o}{B_o}\right) = -\frac{\phi}{B_o}\left(\frac{S_{wij}^k - S_{wij}^{k-1}}{\Delta t}\right) + \phi(1-S_w)\left[\frac{\partial(1/B_o)}{\partial P_o}+\frac{C_r}{B_o}\right]\left(\frac{P_{oij}^k - P_{oij}^{k-1}}{\Delta t}\right)$$

$$\frac{\partial}{\partial t}\left(\frac{\phi S_o}{B_o}\right) = -\frac{\phi}{B_o\Delta t}\left(S_{wij}^k - s_{wij}^{k-1}\right) + \frac{\phi(1-S_w)}{\Delta t}\left[\frac{\partial\left(\frac{1}{B_o}\right)}{\partial P_o}+\frac{C_r}{B_0}\right]\left(P_{oij}^k - P_{oij}^{k-1}\right) \quad (19)$$

Substitute $C_{Poo_i} = \frac{\phi_i\left(1-S_{w_i}\right)}{\Delta t}\left[\frac{C_r}{B_o}+\frac{d(1/B_o)}{dP_o}\right]$ and $C_{swoi} = -\frac{\phi_i}{B_{oi}\Delta t_i}$in (19)

$$\frac{\partial}{\partial t}\left(\frac{\phi S_o}{B_o}\right)_i \approx C_{swoi}\left(S_{wij}^k - S_{wij}^{k-1}\right) + C_{pooi}\left(P_{oij}^k - P_{oij}^{k-1}\right) \quad (20)$$

Discretization of the RHS of (13) for water is given by

$$\frac{\partial}{\partial t}\left(\frac{\phi S_w}{B_w}\right) = \frac{\phi}{B_w}\frac{\partial S_w}{\partial t} + S_w\frac{\partial}{\partial t}\left(\frac{\phi}{B_w}\right)$$

$$\frac{\partial}{\partial t}\left(\frac{\phi S_w}{B_w}\right) = \frac{\phi}{B_w}\frac{\partial S_w}{\partial t} + S_w\left[\phi\frac{\partial(1/B_w)}{\partial t}+\frac{1}{B_w}\frac{\partial\phi}{\partial t}\right]$$

$$\frac{\partial}{\partial t}\left(\frac{\phi S_w}{B_w}\right) = \frac{\phi}{B_w}\frac{\partial S_w}{\partial t} + S_w\left[\phi\frac{\partial(1/B_w)}{\partial P_w}.\frac{\partial P_w}{\partial t}+\frac{1}{B_w}\frac{\partial\phi}{\partial P_o}.\frac{\partial P_o}{\partial t}\right] \quad (21)$$

Using auxiliary equation (6) and substituting for $C_r = \frac{\partial\phi}{\phi\partial P_o}$,

$$P_w = P_o - P_{cow} \quad , \quad \frac{\partial P_w}{\partial t} = \frac{\partial P_o}{\partial t} - \frac{\partial P_{cow}}{\partial t}$$

into equation (21) yields

$$\frac{\partial}{\partial t}\left(\frac{\phi S_w}{B_w}\right) = \frac{\phi}{B_w}\frac{\partial S_w}{\partial t} + S_w\left[\phi\frac{\partial\left(\frac{1}{B_w}\right)}{\partial P_w}\left(\frac{\partial P_o}{\partial t}-\frac{\partial P_{cow}}{\partial t}\right) + \frac{\phi}{B_w}\frac{\partial\phi}{\phi\partial P_o}\frac{\partial P_o}{\partial t}\right] \quad (22)$$

Using backward difference, (22) becomes

$$\frac{\partial}{\partial t}\left(\frac{\phi S_w}{B_w}\right) = -\frac{\phi}{B_w}\left(\frac{S_{wi}-S_{wi}^t}{\Delta t}\right) + S_w\left[\begin{matrix}\phi\dfrac{\partial\left(\frac{1}{B_w}\right)}{\partial P_w}\left(\dfrac{\partial P_o}{\partial t}-\dfrac{\partial P_{cow}}{\partial t}\right)\\ +\dfrac{\phi C_r}{B_w}\end{matrix}\right]\left(\frac{P_{oi}-P_{oi}^t}{\Delta t}\right)$$

$$\frac{\partial}{\partial t}\left(\frac{\phi S_w}{B_w}\right) = -\frac{\phi}{B_{wi}}\left(\frac{S_{wi}-S_{wi}^t}{\Delta t}\right) + \frac{\phi_i S_{wi}}{1}\left[\begin{matrix}\dfrac{\partial\left(\frac{1}{B_w}\right)}{\partial P_w}\left(\dfrac{\partial P_o}{\partial t}-\dfrac{\partial P_{cow}}{\partial t}\right)\\ +\dfrac{C_r}{B_w}\end{matrix}\right]\left(\frac{P_{oi}-P_{oi}^t}{\Delta t}\right)$$

$$\frac{\partial}{\partial t}\left(\frac{\phi S_w}{B_w}\right) = -\frac{\phi}{B_{wi}}\left(\frac{S_{wi}-S_{wi}^t}{\Delta t}\right) + \phi_i S_{wi}\left[\begin{matrix}\dfrac{d\left(\frac{1}{B_w}\right)}{dP_w}\left(-\dfrac{dP_{cow}}{dt}\right)\\ +\dfrac{C_r}{B_w}\end{matrix}\right]\left(\frac{P_{oi}-P_{oi}^t}{\Delta t}\right) \quad (22a)$$

Using

$$C_{Pow_i} = \frac{\phi_i S_{wi}}{\Delta t}\left[\frac{C_r}{B_o}+\frac{d\left(\frac{1}{B_w}\right)}{dP_w}\right]_i$$

$$and\ C_{swwi} = \frac{\phi_i}{B_{wi}\Delta t_i} - \left(\frac{dP_{cow}}{dS_w}\right)_i C_{powi}$$

(22a) becomes

$$\frac{\partial}{\partial t}\left(\frac{\phi S_w}{B_w}\right)_i \approx C_{pow_i}\left(P_{o_i}-P_{o_j}^t\right) + C_{sww_i}\left(S_{w_i} - S_{w_i}^t\right) \quad (23)$$

Substituting equations (15a-15d), (20), (23) in (13) and (14) and rearrange together yields

$$A_x T_{xoi\frac{1}{2},j1}\left(P_{oi+1,j}-P_{oi,j}\right) + A_x T_{xoi-\frac{1}{2},j}\left(P_{oi-1,j}-P_{oi,j}\right) + A_y T_{yoi,j+\frac{1}{2}}\left(P_{oi,j+1}-P_{oi,j}\right) + A_y T_{xoi,j-\frac{1}{2}}\left(P_{oi,j-1}-P_{oi,j}\right) + q_{osc} = C_{pooi}\left(P_{oi}-P_{oi}^1\right) + C_{swoi}\left(S_{wi}-S_{wj}^t\right) \quad (24)$$

$$A_x T_{xwi+\frac{1}{2},j}\left(P_{wi+1,j}-P_{wi,j}\right) + A_x T_{xwi-\frac{1}{2},j}\left(P_{wi-1,j}-P_{wi,j}\right) + A_y T_{ywi,j+\frac{1}{2}}\left(P_{wi,j+1}-P_{wi,j}\right) + A_y T_{xwi,j-\frac{1}{2}}\left(P_{wi,j-1}-P_{wi,j}\right) + q_{wsc} = C_{powi}\left(P_{oi}-P_{oi}^t\right) + C_{swwi}\left(S_{wi}-S_{wi}^t\right) \quad (25)$$

Equation (25) was transformed into oil states only by using the capillary pressure relation equation (6) yields

$$A_x T_{xwi+\frac{1}{2},j}\left[\begin{matrix}\left(P_{oi+1,j}-P_{cowi+1,j}\right)-\left(P_{oi,j}-P_{cowi,j}\right)\\ +A_x T_{xwi-\frac{1}{2},j}\left(P_{oi-1,j}-P_{cowi-1,j}\right)-\left(P_{oi,j}-P_{cowi,j}\right)\end{matrix}\right] + A_y T_{ywi,j+\frac{1}{2}}\left[\begin{matrix}\left(P_{oi,j+1}-P_{cowi,j+1}\right)-\left(P_{oi,j}-P_{cowi,j}\right)\\ +A_y T_{ywi,j-\frac{1}{2}}\left(P_{oi,j-1}-P_{cowi,j-1}\right)-\left(P_{oi,j}-P_{cowi,j}\right)\end{matrix}\right] + q_{wsc} = C_{Pow_i}\left(P_{o_i}-P_{o_i}^t\right) + C_{sww_i}\left(S_{w_i}-S_{w_i}^t\right)$$

$$A_x T_{swi+\frac{1}{2},j}\left(P_{oi+1,j}-P_{oi,j}\right) + A_x T_{xwi-\frac{1}{2},j}\left(P_{oi-1,j}-P_{oi,j}\right) + A_y T_{ywi,j+\frac{1}{2}}\left(P_{oi,j+1}-P_{oi,j}\right) + A_y T_{ywi,j-\frac{1}{2}}\left(P_{oi,j-1}-P_{oi,j}\right) + q_{osc} + ATPC = C_{powi}\left(P_{oi}-P_{oi}^t\right) + C_{swwi}\left(S_{wt}-S_{wi}^t\right) \quad (26)$$

such that

$$ATPC = A_x T_{xwi+\frac{1}{2},j}\left(p_{cowi,J}-p_{coi+1,j}\right) + A_x T_{xwi-\frac{1}{2},j}\left(P_{cowi,j}-P_{cowi-1,j}\right) + A_y T_{ywi,j+\frac{1}{2}}\left(P_{cowi,j}-P_{cowi,j+1}\right) + A_y T_{ywi,j-\frac{1}{2}}\left(P_{cowi,j}-P_{cowi,j-1}\right)$$

In order to determine the initial water saturation terms S_{wi}, equations (24) and (25) were combined by re-arranged and simplified to give:

$$S_{w_i} = S_{w_i}^t + \frac{A_x T_{xoi+\frac{1}{2},j}}{C_{swo_i}}\left(P_{oi+1,j}-P_{oi,j}\right) + \frac{A_x T_{xoi-\frac{1}{2},j}}{C_{swo_i}}\left(P_{oi-1,j}-P_{oi,j}\right) + \frac{A_y T_{yoi,j+\frac{1}{2}}}{C_{swo_i}}\left(P_{oi,j+1}-P_{oi,j}\right) + \frac{A_y T_{xoi,j-\frac{1}{2}}}{C_{swo_i}}\left(P_{oi,j-1}-P_{oi,j}\right) + \frac{q_{osc}}{C_{swo_i}} - \frac{C_{poo_i}}{C_{swo_i}}\left(P_{o_i}-P_{o_i}^t\right) \quad (27)$$

Equation (27) is the solution to (8) and (9) coupled with the auxiliary equations (28), (29), and (30) given by Schneider, (2013).

$$P_c = -BI_n(S_w) = P_o - P_w \quad (28)$$

$$K_{rw} = \left(\frac{S_w-0.195}{0.8}\right)^{4.44} \quad (29)$$

$$K_{ro} = [1-1.8(S_w-0.195)]^2 \quad (30)$$

4. Implementation

The implementation of the solution (equation 27) using MATLAB was based on illustration in Figure 1.

$$\left.\frac{\partial P}{\partial x}\right|_{x=0} = 0 \qquad P_{x=Lx} = P_L = 1000 Psi$$

$$\left.\frac{\partial P}{\partial y}\right|_{y=0} = 0 \qquad \left.\frac{\partial P}{\partial y}\right|_{y=Ly} = 0$$

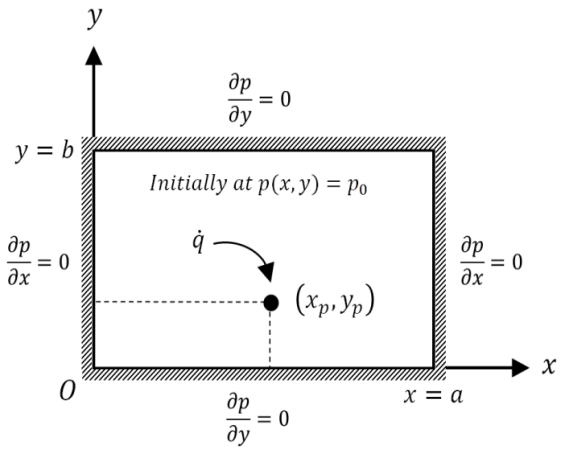

Figure 1: Schematic of a rectangular reservoir with initial and boundary conditions

To produce oil in the upper-right corner, water was injected in the lower left. Using the following initial conditions based on synthetic data obtained from the perturbation of real field data by introducing Gaussian noise of ±10%:

Initial oil pressure P_{oi}= 400 psi
Initial pressure of water injected = 5,000 psig
Initial water saturation S_{wi}=18%
Initial oil saturation S_{oi} = 82%
Sor = Swc = Swirr≥ 25% (Crane, 2018)
Porosity ϕ = 20%
K = 236 md

The pressure and saturation responses obtained from the implementation are as depicted by the characterization signature plots in Figure (2-11).

5. Results and Discussion

5.1 Variations in Reservoir Flow Properties

The characterization signature plots relating saturation and pressure changes to reservoir sensitivityat different simulation times are as depicted in Figure 2-11. The plots indicate significant difference between waterpressure (P_w) 4550 psi(Figure 2a) and oil pressure (P_o) 350 psi (Figure 2b) with corresponding water saturation (S_w) of about 0.73 (Figure 3a) and oil saturation (S_o) of about 0.32 (Figure 3b) at time t = 0.1s. A slight drop in water and oil pressure to 4525 psi (Figure 4a) and 320 psi (Figure 4b) respectively resulted to infinitesimal increase in S_w to 0.732 (Figure 5a) but decrease in S_o to 0.28 (Figure 5b) at time t = 0.25 s.

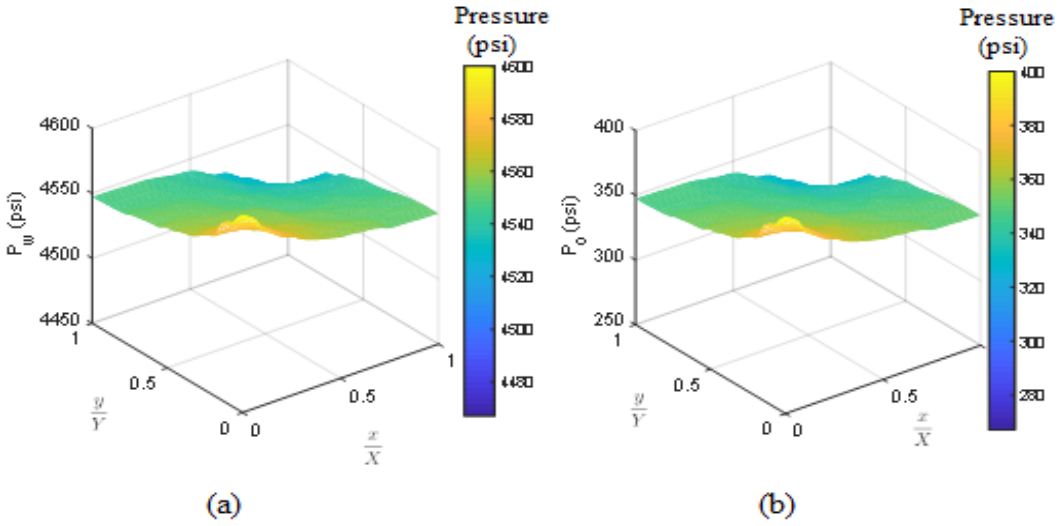

Figure 2: Pressure vs dimensionless distance at time t=0.1s (a) water pressure, (b) oil pressure

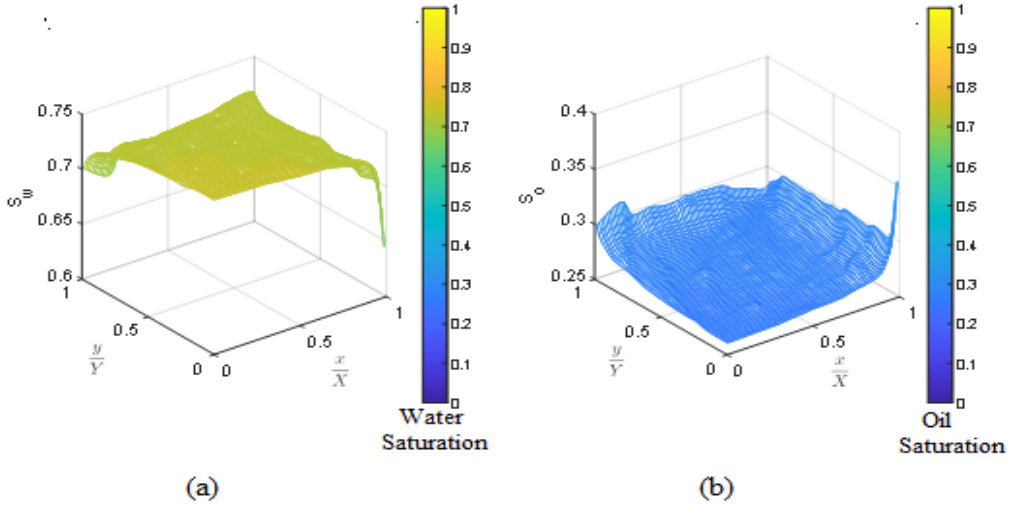

Figure 3: Saturation vs dimensionless distance at time t=0.1s (a) water saturation, (b) oil saturation

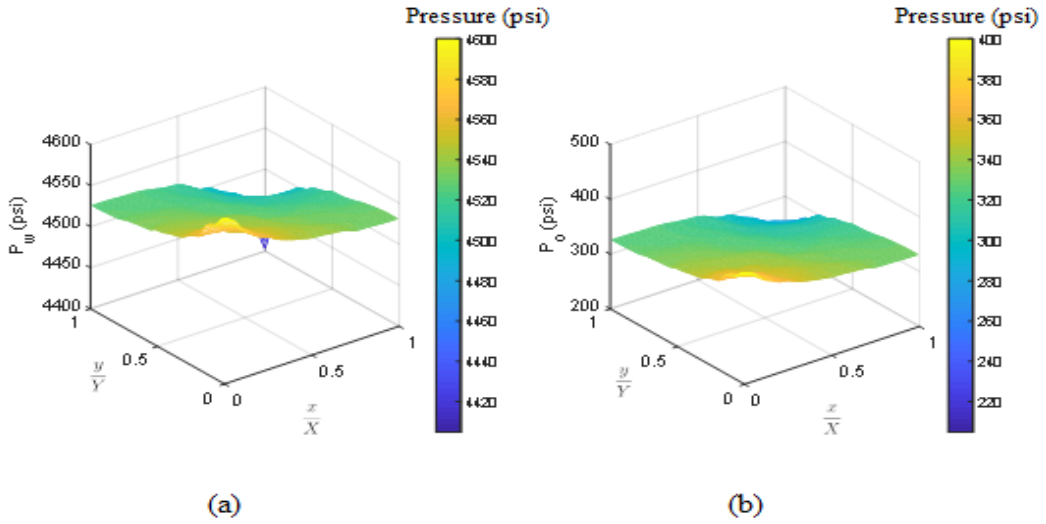

Figure 4: Pressure vs dimensionless distance at time t=0.25s (a) water pressure, (b) oil pressure

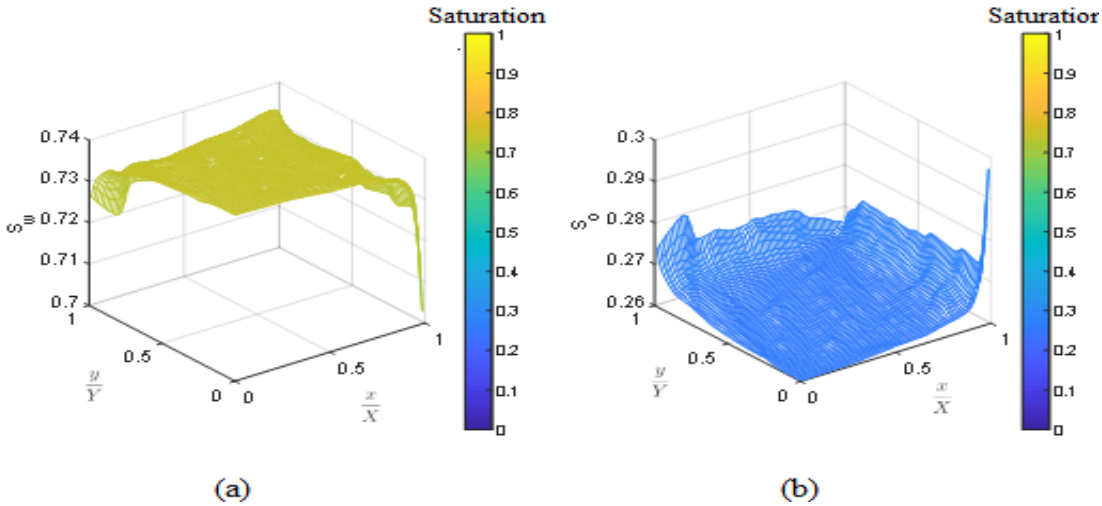

Figure 5: Saturation vs dimensionless distance at time t=0.25 s (a) water saturation, (b) oil saturation

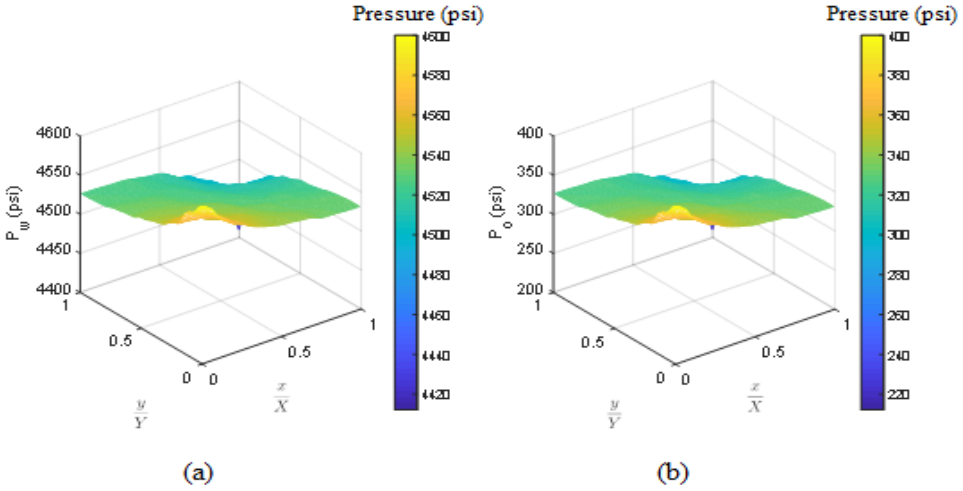

Figure 6: Pressure vs dimensionless distance at time t=0.5s (a) water pressure, (b) oil pressure

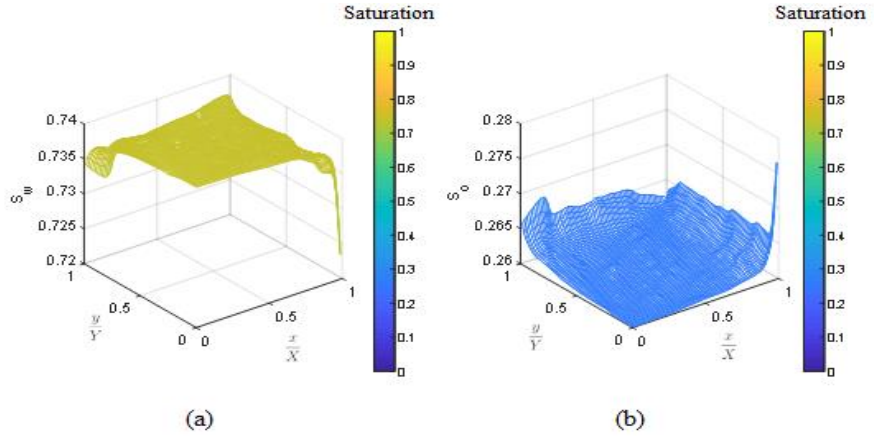

Figure 7: Saturation vs dimensionless distance at time t=0.5s (a) water saturation (b) oil saturation

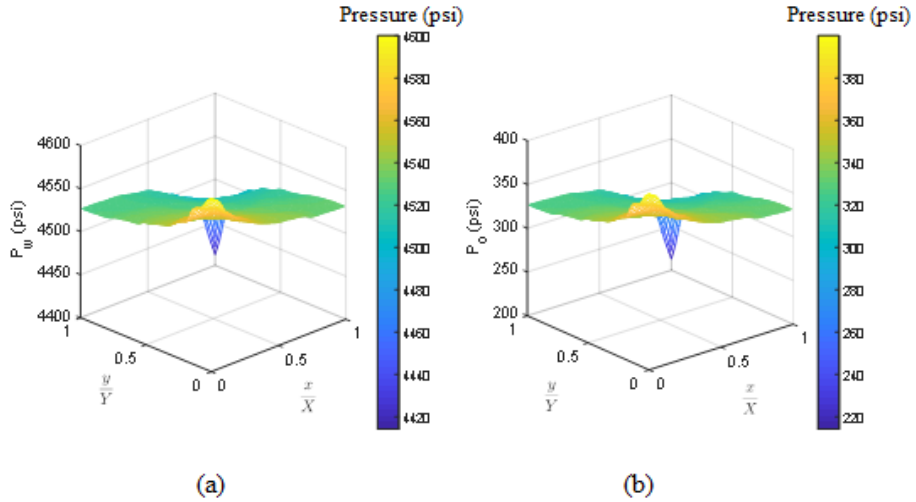

Figure 8: Pressure vs dimensionless distance at time t=0.75s (a) water pressure, (b) oil pressure

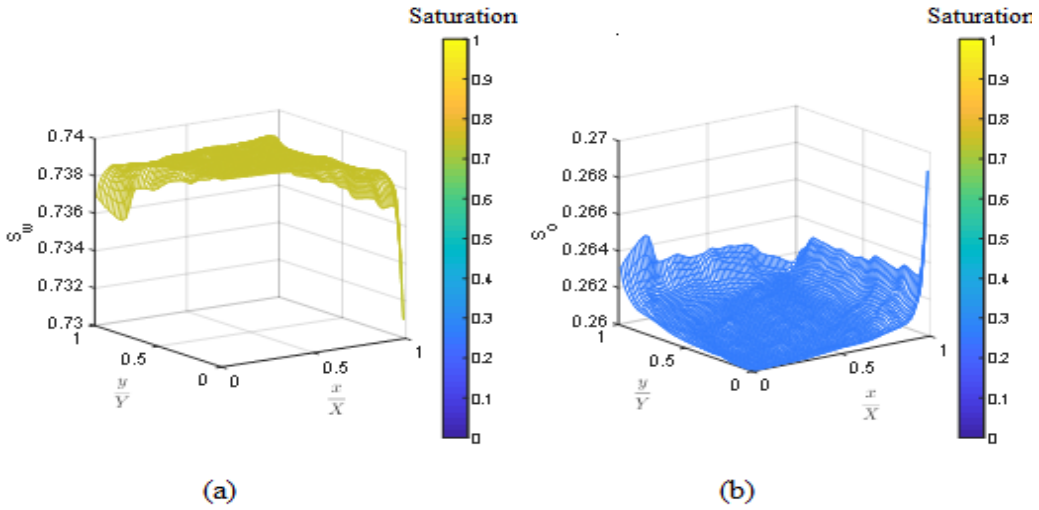

Figure 9: Saturation vs dimensionless distance at time t=0.75 s (a) water saturation, (b) oil saturation

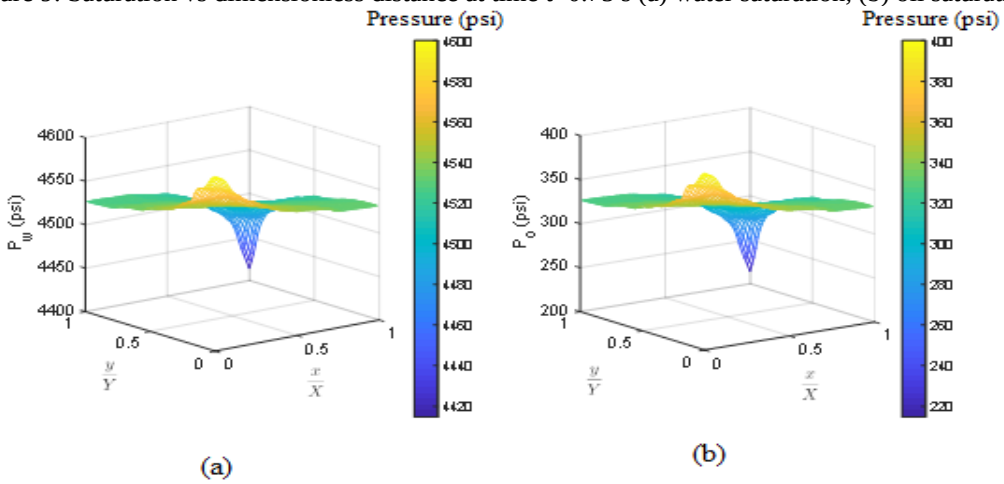

Figure 10: Pressure variations vs dimensionless distance at time t=1.0 s (a) water pressure, (b) oil pressure

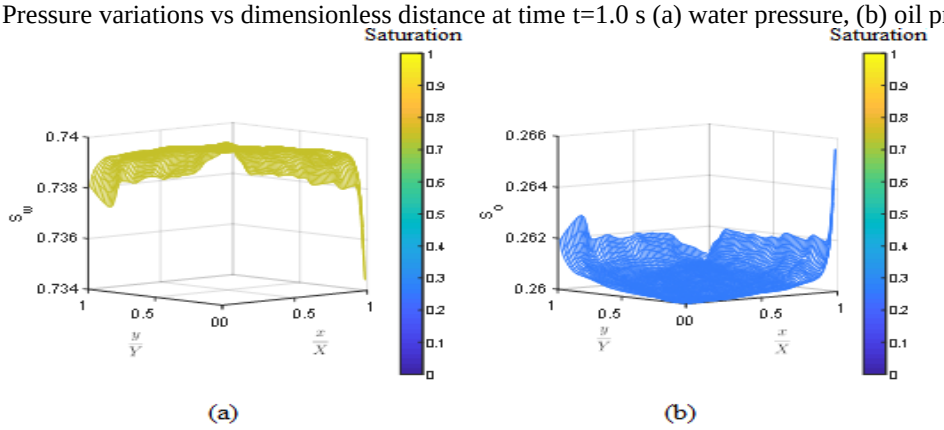

Figure 11: Saturation vs dimensionless distance at time t=1.0 s (a) water saturation, (b) oil saturation

However, there was a slight increase in water and oil pressure to 4530 psi (Figure 6a) and 325 psi (Figure 6b) respectively resulting to corresponding increase in S_w to 0.735 (Figure 7a) and S_o to 0.268 (Figure 7b) at time t = 0.5s. Both water and oil pressure remained 4525 psi and 325 psi respectively at time t = 0.75s (Figure 8) and 1.00s (Figure 10). However, while S_w increased through 0.738 at t = 0.75s (Figure 9a) to 0.739 at t = 1.0s (Figure 11a); S_o decreased through 0.265 at t = 0.75s (Figure 9b) to 0.263 at t = 1.00s (Figure 11b). These indicate fluctuation in water and oil pressure between t = 0.1s and t = 0.50sbut became steady and low at t = 0.75s and t = 1.0s suggesting the reservoir has reached depletion. This was corroborated by decrease in S_o through the entire pressure regime, whereas S_w increased.

5.2 Relative Permeability Curves

In order to investigate the sensitivities of pressure and saturation changes to reservoir porosity and permeability, water and oil saturations from the simulation of equation (27) as revealed by Figure 2-11 were substituted in (29) and (30) to obtain the results for water relative permeability K_{rw} (Figure 12) and oil relative permeability K_{ro} (Figure 13). The relative permeability of water K_{rw} increases with water saturation S_w (Figure 12a) but decreases with increase in oil saturation S_o (Figure 12b).

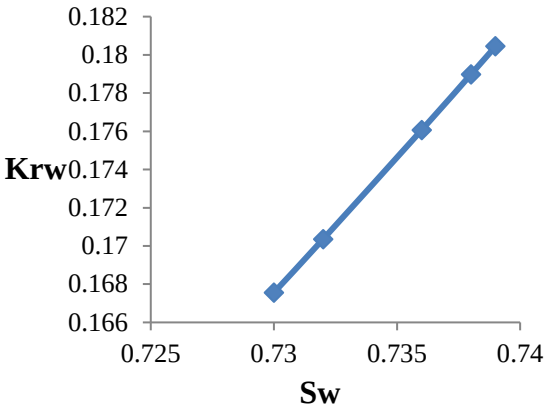

Figure 12a: Relative permeability to water vs water saturation

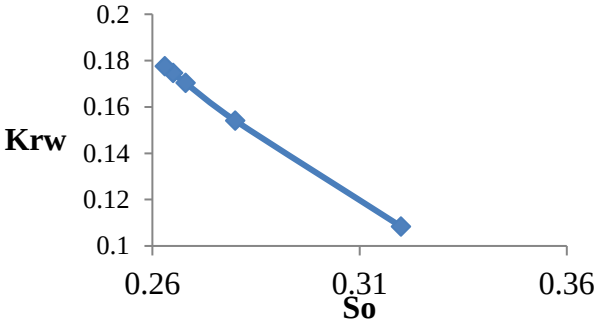

Figure 12b: Relative permeability to water vs oil saturation

On the other hand, while relative permeability of oil K_{ro} decreases with increase in water saturation S_w (Figure 13a), oil saturation S_o increases with K_{ro} (Figure 13b). Thus, as water saturation increases, known as imbibition condition, the oil relative permeability decreases, water relative permeability increases. Conversely, as oil saturation increases (drainage condition), relative permeability of oil increases, relative permeability of water decreases. Generally, however, for every value of either S_o or $S_w, k_{rw} \gg k_{ro}$.

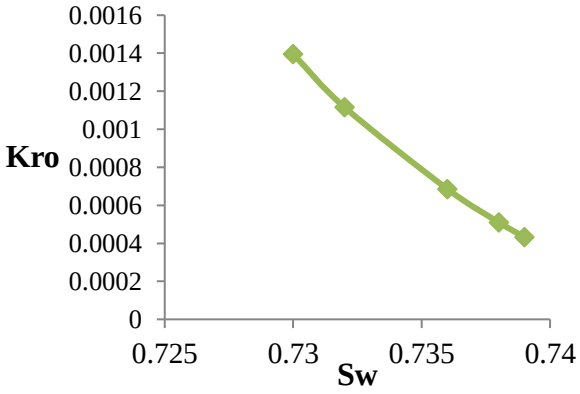

Figure 13a: Relative permeability to oil vs water saturation

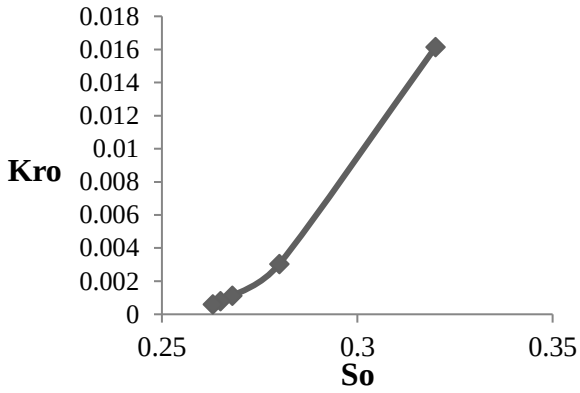

Figure 13b: Relative permeability to oil vs oil saturation

Nomenclature

A	Cross-sectional area	S_{oi}	Irreducible oil saturation	p_{nw}	Non-wetting phase
$ATPC$	Constant denotation	S_{wirr}	Irreducible water saturation	p_w	Water pressure/wetting phase
B_f	Phase formation volume factor	S_{or}	Residual oil saturation	q_{wsc}	Water injection at standard condition
B_o	Formation volume factor for oil	t	Time step	q_{osc}	Oil injection at standard condition
B_w	Formation volume factor for water	v_b	Buck volume	S_w	Water saturation
C_t	Total compressibility	V_x	Flow rate in x-direction	S_o	Oil saturation
C_f	Formation compressibility	V_y	Flow rate in y-direction	λ_w	Water mobility
C_o	Oil compressibility	(x, y, z)	Coordinate system	λ_o	Oil mobility
C_w	Water compressibility	μ	Viscocity	Δx	Change in x
k	Permeability	μ_o	Oil viscosity	Δy	Change in y
k_o	Oil permeability	μ_w	Water viscosity	Δp	Change in pressure
k_w	Water permeability	ρ_w	Water density	ϕ	Porosity
k_r	Relative permeability	ρ_o	Oil density	α	Half-axis ellipsoid
K_{rw}	Relative permeability to water	p	Pressure	k	counter
K_{ro}	Relative permeability to oil	p_c	Capillary pressure	λ	mobility
n	Saturation exponent	p_{cow}	Capillary pressure to oil/water		
		p_o	Oil pressure		

6. Conclusion

Numerical simulation is effective for predicting reservoir behavior, specifically; change in reservoir properties has been simulated by formulating models involving modification of Darcy's equation. The results of formulated and numerically resolved coupled transient linear partial differential equation (CTLPDE) indicated increase in water saturation but decrease in oil saturation throughout the pressure regime of both oil and water which initially fluctuated and subsequently remained constant. The results of the corresponding auxiliary equation indicated increase in relative permeability of water (k_{rw}) with water saturation (S_w) but decreased with increase in oil saturation S_o, while relative permeability of oil (k_{ro}) decreased with increase in S_w but increased with S_o. Generally, however, for every value of either $S_o$or S_w , $k_{rw} \gg k_{ro}$

Numerical simulation proved to be effective in predicting reservoir behavior. The formulated models indicate drop in oil saturation as pressure depleted over time.

7. Acknowledgement

The authors would like to acknowledge the cooperation and support of the NNPC joint operators for the use of some classified information provided.

References

Abreu, E., Furtado, F. and Pereira, F. (2007): Numerical Simulation of Three-Phase flow in Heterogeneous Porous Media; *Seminar Presented in Department of Mathematics*, VECPAR, LNCS, 4395, 504-517.

Amanda, A., Pedro, A. and Lucy M. (2018): Reservoir Lithology and Fluid Properties can be Characterized using Seismic; *CSEM and Rock Physics;* Vol.13, No. 3. Pp. 45-53.

Ayorinde, Rufia and John, P. Crawshaw (2018): Effects of Wettability Changes on Evaporation Rate and the permeability Improvement Due to Salt Deposition; *Journal; ACS Earthand Space Chemistry*,Pp. 21-30.

Cai, J., Hu, X. (2019): Petrophysical Characterization and Transport in Unconventional Reservoirs; Elsevier: Amsterdam, The Netherlands, p.352

Chen, M.; Cheng, L.; Cao, R.; Lyu, C. (2018): A Study to Investigate Fluid-Solid interaction Effects on Micro Scales; *Energies*, 11, 2197.

Civan, F. (2000): Reservoir Formation Damage-Fundamentals, Modeling, Assessment, and Mitigation; 2nd Ed., *Gulf Professional Pub.*, Elsevier, 11-14.

Civan, F. (2001): Scale Effect on Porosity and Permeability-Kinetics, Model, and Correlation*; AICHE J.*, Vol. 47, No. 2, 271-287.

Civan, F. (2002): Relative Permeability to Pore Connectivity using a Power-Law Flow unit Equation; Petrophysics Journal, Vol. 43, No. 6, pp.457-476.

Civan, F. (2003): Reservoir Formation Damage-Fundamental, Modeling, Assessment, and Mitigation; *1st Ed, Gulf Pub*. Co, Houston TX, and Butterworth-Heineman, MA, 74-82.

Civan, F. (2004): Temperature Dependence of Wettability Related Rock Properties Correlated by the Arrhenins Equation;*Petrophysics,* Vol.45, No.4, 350-362.

Civan, F. (2007): Formation Damage Mechanisms and Their Phenomenological Modeling; *SPE-107875*, 2-12.

Civan, F.(2015): Reservoir Formation Damage; 3td Ed. ISBN: 978-0-12-801898-9. *Gulf Professional Pub.,* Elsevier, pp. 11-14.

Lopez, Crucelis C. and Davis, Thomas L. (2011): Permeability Prediction and its Impact on Reservoir Modeling at Postle Field, Oklahoma. *The Leading Edge, Special Section,* ISSN-1070-485X, pp. 80-88.

Ma, H.; Leonard, K.; Herbert, H. (2018): Relative Permeability of Petroleum Reservoirs; CRC Press, Taylor & Francis Group. New York. Pp. 25-30

Marcelo, D. Queiroz, E. and Paulo C. (2013): A general Analytic Solution for theMultidimensional Hydraulic Diffusivity Equation by Integral Transform Technique; *OTC 24319*.

Schneider, J. H. (2013): Empirical Capillary Relationship; *Consulting Reservoir Engineer*, Poteet, Texas, U.S.A.

Wang, Y.; Chen, B.; Ren, S.; Zhang, L.;and Cui, G (2018): Assessing the combined influence of fluid-rock interaction on reservoir properties and injectivity during CO_2 Storage in Saline Aquifers; *Energy-Elsevier* Vol.155, pp. 281-296.

Wyllie, M. R. J. and Rose, W. D. (1950): Some Theoretical Consideration Related to the Quantitative Evaluation of the Physical Characteristics of Rock from Electric log Data; *Journal of Petroleum Technology*, 189: 105-110.

Xu, Z.; Zhao, P.; Wang, Z.; Ostadhassan, M.; Pan, Z. (2018): Characterization and Consecutive Prediction of Pore Structures in Tight Oil Reservoirs; *Energies*, 11, 2705.